Stanisław F. ŚCIESZKA[*], Marcel ŻOŁNIERZ[*]

STUDY ON THERMO-MECHANICAL INSTABILITY IN THE INDUSTRIAL BRAKES

BADANIA TERMOMECHANICZNEJ NIESTABILNOŚCI HAMULCÓW PRZEMYSŁOWYCH

Key words:

industrial brakes, thermal stress, friction characteristics, disc distortion

Słowa kluczowe:

hamulce przemysłowe, naprężenia termiczne, chatakterystyki tarcia, deformacja dysku

Summary

This paper presents disc brake surface temperature field measurements, during emergency braking in real industrial conditions, by means of the thermovision infrared camera. The temperature field assessment enables the verification of the numerical modelling of the brake performance in the succeeding step. The experimental part of the research also covers tribological testing on the coefficient of friction between the friction brake material (brake pad) and steel (brake disc) in laboratory conditions on a tribotester which satisfied the similarity criteria with the mine winder hydraulic disc brake. The tribological

[*] Politechnika Śląska, Wydział Górnictwa i Geologii, Instytut Mechanizacji Górnictwa, ul. Akademcka 2, 44-100 Gliwice.

characteristic of the friction couple, including the kinetic and static coefficients of friction, were determined for use in the finite elements analysis (FEA) of the brake thermo-mechanical instability (TMI) problem.

In the numerical part of this work, the FE modelling technique was used to simulate the brake interface hot spotting and the axial disc distortion as a function of the geometrical and material properties of the brake elements and the brake's operational conditions. The critical speed above which TMI would occur was calculated for the analysed mine winder brake system.

A FE method was used to find the temperature distribution and the resulting thermal stresses and distortions in the brake discs. The disc division into various numbers of sections was numerically tested for the division's effect on thermal stress reduction and axial distortions.

INTRODUCTION

Hot spotting and thermal judder were recorded **[L. 1–3]** during the action of the automotive and railway disc brakes. The most important cause that contributes to both effects is the thermoelastic deformation of the disc **[L. 4–8]**. Thermo-mechanical instability (TMI) in friction disc brakes is the final effect of the a sequence of events, namely, heat generation during friction, and expansion of the disc material leading to an axial deflection of the disc, which in turn increases pressure diversification along the friction surface (pads versus disc friction contact) and consequently diversifies heat generation, temperature distribution (hot spotting) and finally intensifies the disc thermoelastic stresses and deformations.

The above statements was confirmed by numerous experimental investigations on automotive and railways disc brakes and by many finite element analyses (FEA) of the magnitude and distribution of the brake disc temperature **[L. 5–10]**. For each brake system, there is a critical value of sliding velocity, v_{cr}, above which hot spotting takes place **[L. 6]**. In works concerning automotive disc brakes, the borderline between thermoelastic stability and instability was established based on the temperature difference between both sides of the disc. Determination of the critical velocity, v_{cr} according to the assumption made in **[L. 7]** might be related to over a 10% differentiation in temperature on the opposite sides of the disc. For the given friction, disc brake velocity higher then v_{cr} is going to initiate thermoelastic instability.

This criterion appeared to be inappropriate for the very large industrial disc brakes. The winder's brakes, contrary to automotive brakes, distinguish themselves by a very large diameter of the disc (in some cases over 6 meters) and a relatively small gap between pads and disc (axial clearance is usually between 1.5 to 2.0 mm). The slackness of the gap and journal bearings both sharply limit the permissible axial deformation of the disc. The critical permissible axial deformation of the disc might be considered as the new

criterion for thermo-mechanical instability (TMI) determination in industrial brakes **[L. 11]**.

Alternative criterion that might be crucial in establishing the critical braking conditions (e.g. critical velocity, v_{cr}) is related to the thermal stresses generated in the disc during the winder's emergency braking. It has been reported **[L. 12, 13**] that, for non-divided disc (disc in one piece joined to the multi-rope drum by fitted bolts), maximal thermal stresses are higher than the yield strength of the steel used to manufacture the disc.

INFRARED INVESTIGATION OF WINDER DISC BRAKE DURING EMERGENCY BRAKING

The winder emergency braking is carried out by a mechanical friction brake, which in various operational situations, becomes the ultimate means of retardation for the winding system. The emergency braking might be initiated, e.g., at maximum speed, whenever power or control is lost. The objective of this solely friction braking is stopping the winder before conveyance reaches the limits of travel. Infrared investigations covered emergency stopping from maximum speed to zero on the mine winder. The most important technical parameters are listed in **Table 1.**

Table 1. Technical data of the mine winder
Tabela 1. Parametry techniczne hamulca maszyny wyciągowej

N^o	Parameter	Symbol	Unit	Value
1	Initial velocity (maximal)	v_m	$m \cdot s^{-1}$	10
2	Deceleration (nominal)	b	$m \cdot s^{-2}$	1.52
3	Breaking force (total)	P_h	N	299127
4	External disc radius	R_2	m	1.925
5	Internal disc radius	R_1	m	1.450
6	Disc thickness	b_1	m	0.022
7	Number of discs	i	-	1
8	Number of disc's segments	s	-	4
9	Disc's mass	m_1	kg	888
10	Brake pad length	l_2	m	0.3
11	Brake pad width	g_2	m	0.22
12	Brake pad thickness	b_2	m	0.027
13	Number of brake callipers	i_2	-	6
14	Hoisting depth	h	m	984
15	Number of hoisting ropes	L_h	m	4
16	Number of hoisting balance ropes	L_b	m	2

In the investigation of the surface temperature distribution on the brake disc, a thermovision camera **(Fig. 1)** was used.

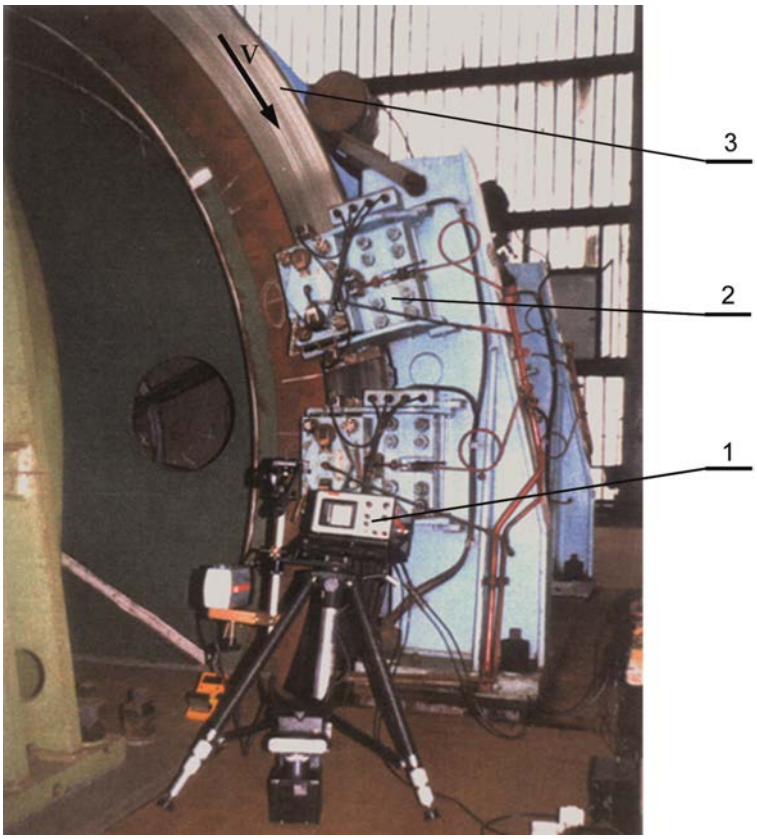

Fig. 1. View of workplace for thermovision investigation. 1 – thermovision camera, 2 – calliper hydraulic brake, 3 – disc (outside diameter Ø 4 m)

Rys. 1. Widok stanowiska do pomiarów termowizyjnych, gdzie: 1 – kamera termowizyjna, 2 – siłownik hydrauliczny, 3 – tarcza (średnica zewnętrzna Ø 4 m)

The camera's zoom lens enabled a field of view on the disc equal 0.32 x 0.32 m^2 from a distance of 1 metre. The surface temperature distribution during the winder's emergency braking was recorded as a function of the brake action time. The emissivity of the disk surface was experimentally determined **[L. 14]** by a comparison of the infrared camera results with temperature test measurements by the thermocouples placed in selected points on the disc surface. The friction surface of the disc has diversified emissivity because of a circular-strip like micro-roughness structure, which was formed mainly by frictional action of hard particles of brake pad's composite (NAO – non-

asbestos organic) material **[L. 15]**. Scatter of the emissivity results and the spread of averages on the tribologically active part of the disc surface are represented by the following:

$$\bar{\varepsilon} = 0,49 \text{ – arithmetic mean value}$$

and

$$s(\varepsilon) = 0.025 \text{ – standard deviation}$$

The applications of the thermovision measuring system for the experimental research of the brake disc-surface-temperature field during braking were presented in **[L. 11]**. Temperature recording was always turned on before braking action began and was terminated after the moving disc came to rest.

The part of disc was observed that was just coming out of frictional contact with the pads (brake linings), **(Fig. 1)**. The results of testing are presented in the form of polychromatic thermograms **(Fig. 2)** and as a numerical data in **Table 2.** Numerical surface temperatures of the discs were evaluated at four measuring points (P1, P2, P3, and P4) arranged along a radius with a distance between them of approximately 70 mm, which made them representative for the whole active width of the disc.

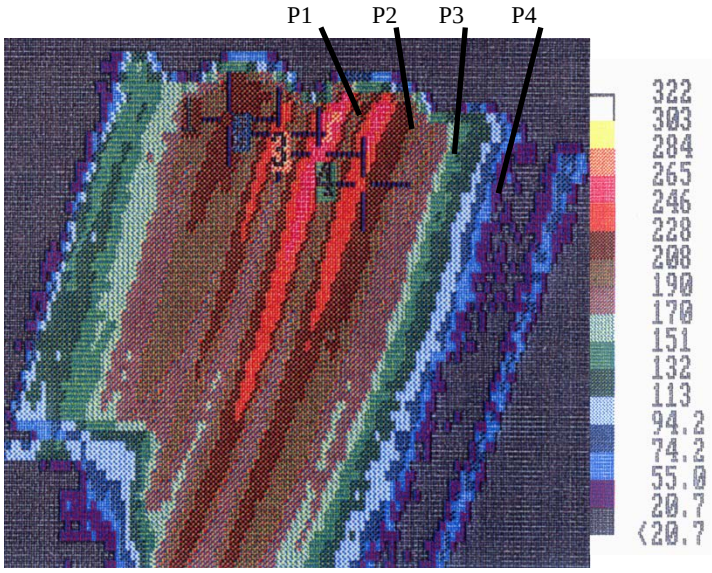

Fig. 2. Thermogram of the disc area during emergency breaking from initial velocity 10 $m \cdot s^{-1}$ just coming out of the frictional contact with brake pads, were P1, P2, P3 and P4 are four measuring points

Rys. 2. Termogram powierzchni tarczy hamulcowej podczas hamowania bezpieczeństwa maszyny wyciągowej z prędkości początkowej 10 $m \cdot s^{-1}$ tuż po wyjściu ze strefy tarcia z okładziną cierną, gdzie P1, P2, P3 i P4 są punktami pomiarowymi

Table 2. Disc surface temperature in ^{o}C during winder emergency breaking, from initial velocity 10 m·s^{-1}, and duration of braking: 5s (emergency braking was initiated during winder operation and values of the initial temperature, for t_o = 0s, were random)

Tabela 2. Temperatura powierzchni tarczy w ^{o}C podczas hamowania bezpieczeństwa maszyny wyciągowej z prędkości początkowej 10 m·s^{-1} i czasie hamowania 5s (hamowanie bezpieczeństwa było inicjowane podczas pracy urządzenia wyciągowego i temperatury początkowe dla t_o = 0s były losowe)

Measuring point	Braking time, s					
	0	1	2	3	4	5
P1	79	132	223	223	208	132
P2	75	151	254	268	279	185
P3	81	135	288	288	259	203
P4	80	104	240	247	250	179

TRIBOLOGICAL CHARACTERISTICS OF THE FRICTION COUPLE BRAKE MATERIAL VERSUS STEEL

Composite friction brake material belonging to the non-asbestos organic (NAO) materials consists of four main components: organic binder (phenolic resin), structural materials (non-asbestos fibers), fillers, and friction modifiers **[L. 3, 15]**. Tribological investigations were conducted in order to determine numerical values of the kinetic and static coefficients of friction between the brake material and disc made out of medium-carbon steel. Tribological characteristics of the friction couple were implemented for FEM analysis of the TMI problem.

Tribological testing was conducted on a braking tribometer **(Fig. 3),** which satisfied the principal tribological similarity criteria with the mine winder hydraulic disc brake, including sliding velocity, mean contact pressure, and surface temperature distribution. The main operational parameters of the tribometer are shown in **Table 3.**

In order to cover the range of temperatures up to 300 ^{o}C, the braking tribometer was equipped with an electric heater used to control the temperature of the disc, particularly during static friction testing. Friction material cylindrical samples (ø24x15 mm) were cut out from randomly selected parts of the brake lining. Before friction testing, the samples were run-in on a distance of about 5000 m in order to achieve uniform distribution of real contacts on the nominal friction surface. During friction testing, the following values were recorded with a 10 Hz frequency: friction force, normal forces between the samples and disc, temperature on the friction surface, and the time of braking action. Approximately 400 tests were carried out for every combination of parameters shown in **Table 3**. The coefficient of static friction was determined on the same tribometer **(Fig. 3)** with the same set of friction material samples. In the designed brake under investigation, the proposed nominal pressure in the frictional interface is equal to

1 MPa; therefore, the brake couple characteristics actually implemented into FEA were limited to such pressure and are presented in **Figs. 4** and **5.**

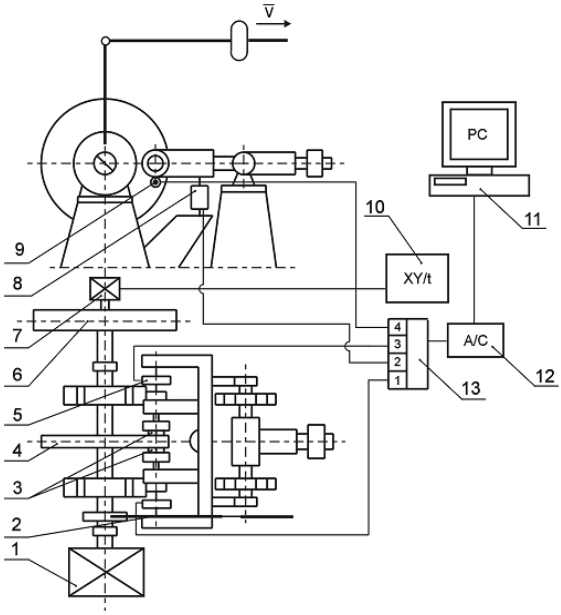

Fig. 3. Braking tribometer diagram and simplified scheme of measuring system. 1 – the DC motor (used for kinetic friction determination), 2 – wrapping connector (used for static friction determination), 3 – friction material sample (pin), 4 – disc, 5 – normal force transducer, 6 – flywheel, 7 – speed indicator, 8 – friction force transducer, 9 – temperature sensor (thermocouple), 10 – voltmeter, 11 – PC-based data acquisition system with a sampling rate of 10 Hz, 12 – fast A/D card, 13 – clamps

Rys. 3. Schemat stanowiska bezwładnościowego do badań tarcia statycznego i kinetycznego, gdzie: 1 – silnik elektryczny (do badań tarcia kinetycznego), 2 – cięgno napędu tarczy (do badań tarcia statycznego) 3 – próbki, 4 – tarcza hamulcowa, 5 – czujnik siły typu CL 16 do pomiaru siły nacisku, 6 – masa bezwładnościowa, 7 – prądnica tachometryczna, 8 – czujnik siły typu CL 14 do pomiaru siły tarcia, 5 – czujnik temperatury typu IT-CC, 10 – woltomierz, 11 – komputer klasy PC, 12 – karta A/C, 13 – panel zacisków śrubowych

Table 3. The tribometer description and its main operational parameters

Tabela 3. Podstawowe parametry stanowiska badawczego

N^o	Parameter	Symbol	Value	Unit
1	Sliding velocity	v	10; 20; 30	$m \cdot s^{-1}$
2	Mean contact pressure	p_n	0.8, 1.0, 1.2, 1.6	MPa
3	Initial temperature of the disc	T_p	50, 150, 300	^oC
4	Pin friction surface	a_2	5.7	cm^2
5	Disc dimension	D, g	Ø320x20	mm
6	Disc friction surface	a_1	200	cm^2
7	Mean friction radius	r	140	mm
Loading system – hydraulic actuators				

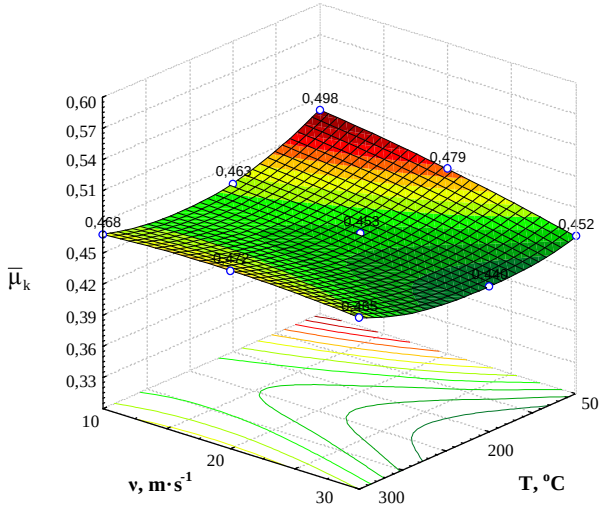

Fig. 4. Kinetic friction characteristics for the brake material (NAO) versus steel disc for various velocities of sliding v, and friction surface temperature T, tested in nominal pressure condition p_n = 1.0 MPa

Rys. 4. Przebieg zmian współczynnika tarcia kinetycznego dla materiału kompozytowego NAO w zależności od prędkości poślizgu (v) i temperatury na powierzchni tarczy hamulcowej T, przy nacisku jednostkowym p_n = 1,0 MPa

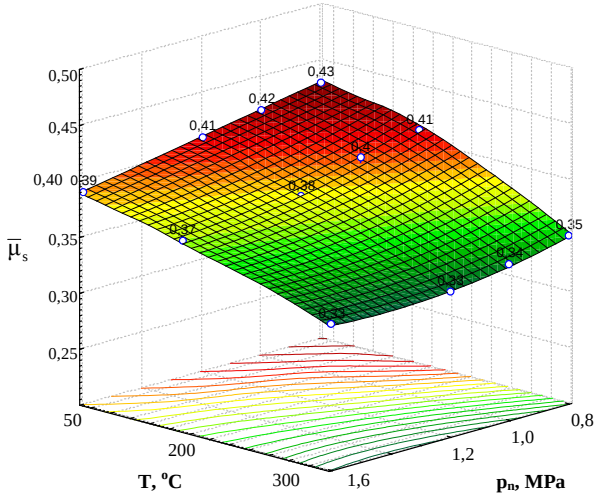

Fig. 5. Static friction characteristics for the brake material (NAO) versus steel disc for various surface temperature T and nominal pressure conditions p_n, (only results for p_n = 1.0 MPa were implemented into FEA)

Rys. 5. Przebieg zmian współczynnika tarcia statycznego dla materiału kompozytowego (NAO) w zależności od temperatury na powierzchni tarczy hamulcowej T i nacisku jednostkowego p_n (tylko wyniki dla p_n = 1,0 MPa zostały uwzględnione w MES)

NUMERICAL MODELLING OF WINDER MACHINE'S EMERGENCY BRAKING BY FEA

Numerical model of the disc brake

Finite elements (FE) modelling was used in the thermal analysis of automotive, railway and industrial brakes **[L. 2, 6, 8, 11, 14, 16].** Application of FE modelling enables relatively extensive simulation of the design features, materials characteristics, and tribological parameters that influence brake performance. Thermal analysis of the brake requires the assessment of the friction energy generated during the braking process. The coefficient is used for the assessment in which the value is equal to about 0.9 according to Taylor and Warren **[L. 17].** Moreover, the heat entering the disk and pad respectively is essential. The heat partition ratio is explained and defined in **[L. 8, 18, 19].** In addition, the disc is cooled by the surrounding air. The cooling process depends on the surrounding temperature and on the rotational speed of the disc. Both, the natural heat convection and forced convection, are taken into consideration in FE modelling.

Frictional heat flux, q, generated in the interface of the brake pair is dependent upon the coefficient of friction, μ, pressure distribution in the brake pair interface, p, and the velocity of the disc brake, v, which decrease with time, hence Equation (1):

$$q(x, y, t) = \mu p v(x, y, t) \tag{1}$$

FEM's are suitable for numerical calculation of stationary elements; however, the three-dimensional modelling of movable elements requires the application of very fine FE mesh. It is related to numerical instability problems when Peclet's number, Pe>2. As the FE results vary slightly, several μm of length must be used, as shows Equation (2):

$$h_x = \frac{\mathrm{Pe} \cdot \lambda}{v \rho c_p} \tag{2}$$

Where: h_x is FE size along velocity vector,
v is sliding velocity,
ρ is disc material's density,
c_p is disc material's specific heat,
λ is disc material's heat transfer coefficient,
Pe is Peclet's number.

In order to shorten computation time, a hybrid method was introduced **[L. 17],** which combines the fast Fourier transformation technique (FFT) with

FEM. To solve the question of heat convection and thermal diffusion, the Petrov-Galerkin method was used **[L.** 20]. Numerical stability of the computation is reached if Courant's number Cu≤1. The value of the Courant's number is calculated from Equation (3):

$$Cu = \frac{v \cdot \Delta t}{h_x} \tag{3}$$

Cu is Courant's number,
Δt is iteration time.

The network applied was not as fine as required by the FE analysis because of limited capacity of the available computing system. The FE model of the brake system (**Fig. 6**) was built from hexahedron, 8-nudal 3D elements (full integration & Herrmann formulation) and subsequently the following appropriate material properties and boundary conditions were set (**Table 4**) and incorporated:

- initial rotational velocity of the disc,
- initial temperature of the model's elements,
- steady temperature of the environment,
- steady pressure in the brake pair interface,
- real rotating and reciprocating winder's masses,
- natural and forced convection,
- thermo-mechanical disc's material dependence on temperature **[L. 11]**, and
- the coefficient of friction dependence on velocity and temperature **(Fig. 4** and **5)**.

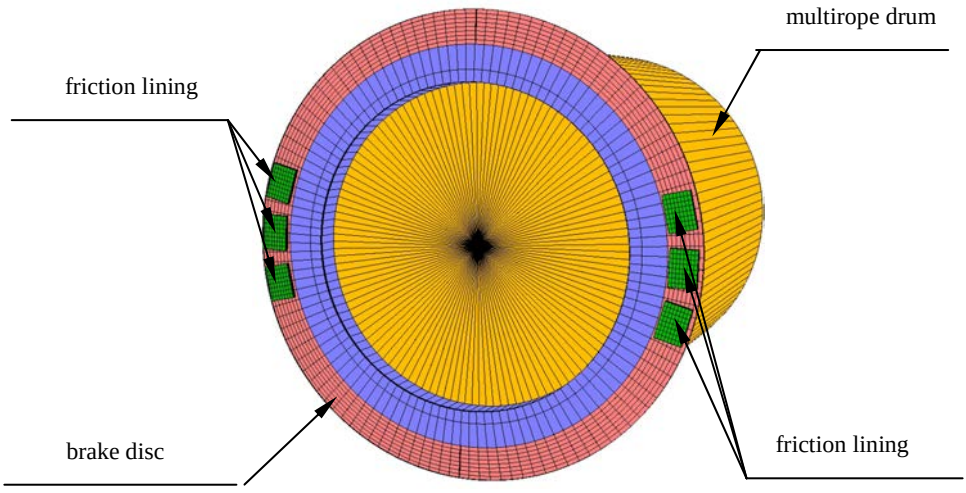

Fig. 6. FE model of the disc brake system
Rys. 6. Model MES hamulca tarczowego maszyny wyciągowej

Table 4. Basic material properties and boundary conditions used in FEA
Tabela 4. Podstawowe warunki brzegowe oraz własności materiałowe tarczy hamulcowej i okładziny ciernej użyte w analizie MES

Parameters and materials properties	Unit	Brake disc	Friction material
Elastic modulus, E	MPa	f(T), **[L. 8]**	$2\cdot10^{8}$
Heat capacity, c_p	$\frac{J}{kg\cdot K}$	f(T), **[L. 8]**	1000
Thermal conductivity, λ	$\frac{W}{m\cdot K}$	f(T), **[L. 8]**	0.3
Thermal expansion coefficient, α	$\frac{1}{K}$	f(T), **[L. 8]**	$2\cdot10^{-5}$
Density, ρ	$\frac{kg}{m^3}$	7850	2000
Temperature of the environment, T_o	^oC	22	
Initial temperature of the disc brake, T_p	^oC	50	
Coefficient of friction	–	f(T, v, p) Fig. 4 and 5	
Pressure in the brake interface, p	MPa	1.0	
Initial sliding velocity, v_o	$M\cdot s^{-1}$	10	

To validate the numerical model, a statistic analysis was used integrated with STATISTICA software. This stage of FEA model verification was described in **[L. 11]**.

Setting limitations on of the thermo-mechanical stability based on criterion concerned with temperature differentiation on opposite sides of the disc

After **[L. 7]**, the criterion of a 10% temperature discrepancy on opposite sides of the disc was accepted as the borderline, and the critical velocity, v_{cr}^{T} initiating thermo-mechanical instability (TMI) was set. Based on the numerical disc brake model **(Fig. 6)** and material properties **(Table 4)**, the dimensionless critical velocity $v_{cr\_dl}^{T}$ and linear critical velocity v_{cr}^{T} were computed. The disc material properties (Table 4) effects on the both critical velocities are shown in **Fig. 7**. Ratio, $\frac{z}{z_0}$, means $\frac{\alpha}{\alpha_0}$, $\frac{E}{E_0}$ and $\frac{\left(\frac{1}{c}\right)}{\left(\frac{1}{c_0}\right)}$ where: α_0, E_0 and c_0 are basic properties of the brake disc material, whereas α, E and c are multiples and fractions of the basic values.

The dimensionless critical velocity was calculated from Equation (4):

$$v_{cr\_dl}^{T} = v_{cr}^{T}\frac{\rho_{01}\cdot c_{01}}{\lambda_{01}}b_1 \tag{4}$$

Where: v_{cr}^{T} – linear critical velocity, $m\cdot s^{-1}$,
ρ_{01} – density of the disc material; 7850 $kg\cdot m^{-3}$,

c_{01} – heat capacity of the disc material at T = 20°C; 486 J · kg^{-1} · K^{-1},
λ_{01} – thermal conductivity of the disc material at T = 20°C; 51,9 W · m^{-1} · K^{-1},
b_1 – brake disc thickness (0,015 m, 0,022 m, 0,03 m).

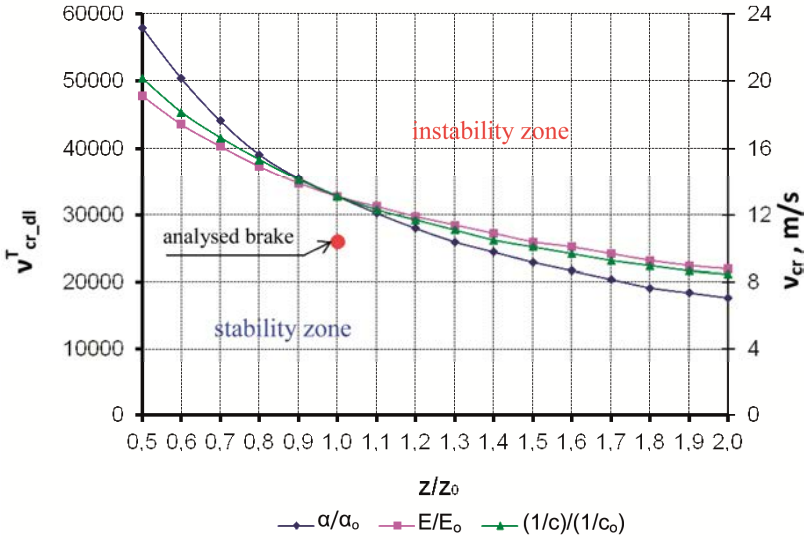

Fig. 7. The effect of the disc material properties on the critical velocity, for the disc thickness b_1 = 0.022 m

Rys. 7. Wpływ własności materiału tarczy na prędkość krytyczną dla grubości tarczy b_1 = = 0,022 mm

Fig. 7 shows both critical velocity changes vs. disc material properties (α, E, c) changes. Graphs obtained from calculations (in accordance with the criterion) determine the instability zone **(Fig. 7).** The strongest effects on the thermo-mechanical stability demonstrate the material thermal expansion, α, of the disc **(Fig. 7).**

Graphs show that the analysed disc brake is situated in stability zone during its nominal performance, i.e. the brake maximal (initial) velocity is 10 m·s^{-1}; whereas, the calculated critical velocity v^T_{cr} = 13 m·s^{-1}. The critical velocity depends on disc thickness **(Fig. 8)** and has highest values for thickest disc, b_1 = 0.03 m, that is, an increase of disc thickness reduces the probability of TMI occurrence.

Industrial and laboratory scale testing as well as FE analysis demonstrated that the surface temperature has not exceeded the permissible temperature for NAO lining material **[L. 3, 11].**

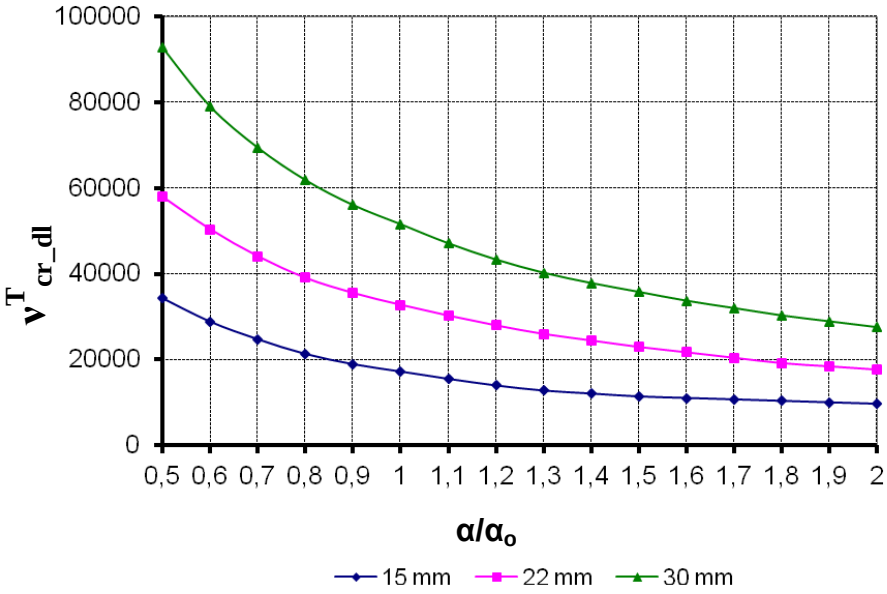

Fig. 8. The effect of thermal expansion of disc material on the dimensionless critical velocity, for disc thickness b_1 = 0.015 m, 0.022 m, 0.03 m

Rys. 8. Wpływ rozszerzalności cieplnej materiału tarczy hamulca na bezwymiarową prędkość krytyczną dla trzech grubości tarczy b_1 = 0,015 m, 0,022 m, 0,03 m

Setting limitation of the thermo-mechanical stability based on criterion concerned with permissible value of the axial brake disc distortion

Because the analysed industrial disc brake does not exceed the stability zone according to the criterion presented above, a new criterion was implemented in order to determine its performance. The new criterion was concerned with the size of the gap between disc and pad (lining) when the brake is disengaged. The size of the gap and allowable main journal bearings axial slackness (axial clearance) determine the critical axial distortion. The maximum size of the gap is determined by Belleville spring pack characteristics and is usually about 1.5–2.0 mm, while the axial slackness of the bearings might be estimated for about 0.3 mm. Therefore, the permissible value of the axial distortion of the disc is approximately 1.2 mm.

Setting the limitation of the thermo-mechanical stability of the analysed industrial brake means computing the initial emergency braking velocity v^d_{cr} which is generating axial disc distortion, a^d (on its external diameter) of about 1.2 mm. Numerical analysis was conducted similarly to the last one (section 4.2).

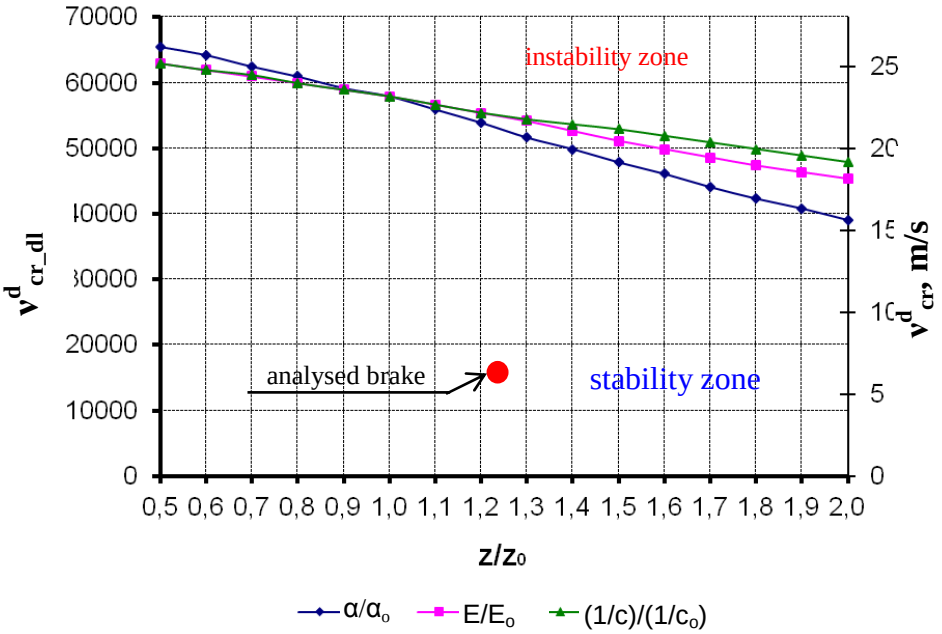

Fig. 9. The effect of the disc material properties on the critical velocity, for the disc thickness b_1 = 0.022 m

Rys. 9. Wpływ własności materiału tarczy hamulca na prędkość krytyczną dla grubości tarczy b_1 = 0,022 m

Figure 9 shows critical velocity ($v^d_{cr\_dl}$ and v^d_{cr}) changes vs. disc material properties (α, E, c). The graphs were obtained from computing the determined stability and instability zones. The dimensionless critical velocity $v^d_{cr\_dl}$ was calculated from Equation (5):

$$v^d_{cr\_dl} = v^d_{cr} \frac{\rho_{01} \cdot c_{01}}{\lambda_{01}} b_1 \tag{5}$$

Where: v^d_{cr} – linear critical velocity, m · s^{-1}.

Figure 9 shows that the both critical velocities are higher than the critical velocities calculated in accordance with previous criterion (section 4.2).

Effect of the disc division on its state of strain and stress

Discs divided into two or four sections are typically used in mines. The discs' division is applied in order to reduce stress during emergency braking. The FE

method was used to find the temperature distribution, the resulting thermal stresses and distortions in the brake discs. The disc division into various numbers of sections was numerically tested for the division's effect on the thermal stress reduction and the axial distortions. FEA found that the bigger the number of sections, the lower the stress. On the other hand, the division of the disc increases the maximal axial distortion of the disc (disc coning). **Fig. 10** shows that, during emergency braking, local stresses of the disc are much closer to the yield strength of the disc's material than the axial disc distortions are to the permissible value of the disc distortion. In analysed industrial brakes, it is more likely that the permissible value of stress (yield strength) is going to be locally exceeded than the permissible value of axial distortion of the disc.

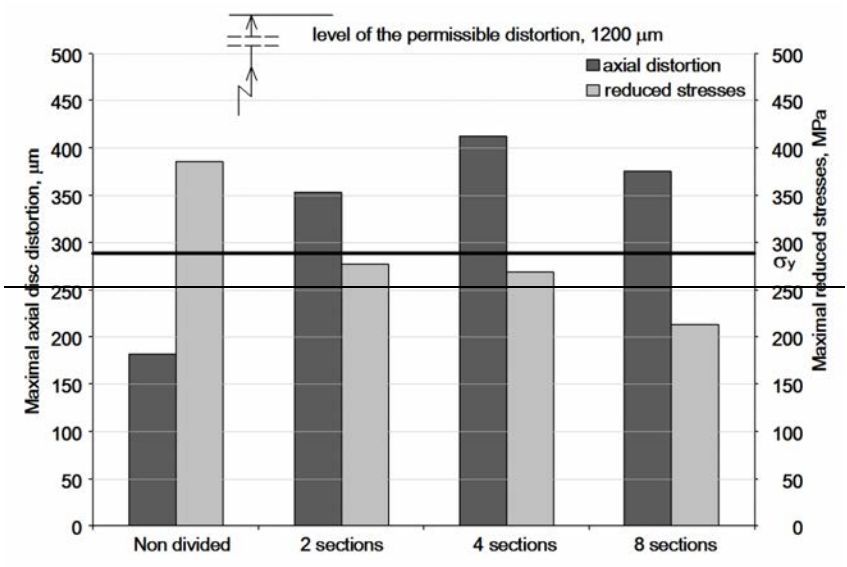

Fig. 10. Maximal axial disc distortions and maximal reduced stresses, for discs divided into various numbers of sections, where σ_y – yield strength of the disc's material

Rys. 10. Maksymalne deformacje osiowe i maksymalne naprężenia zredukowane dla tarczy hamulcowej podzielonej na segment, gdzie σ_y – granica plastyczności materiału tarczy hamulca

CONCLUSIONS

In this article, a novel method for predicting thermo-mechanical instability in friction brakes has been presented and discussed. The results can be concluded as follows.

- FE enables the computing of thermo-mechanical stability zone for every industrial brake system that is defined by the critical velocity above which instability would occur.
- The critical velocity values might be calculated using two criteria. The first is concerned with 10% temperature differentiation on opposite side of the disc, and the second concerned with permissible value of the axial distortion. The second criterion permits higher initial velocity during emergency braking.
- The disc's material thermal expansion coefficient has the strongest influence on the critical velocity. An increase of the thermal expansion coefficient and Young's modulus reduce the value of the critical velocity, which means that TMI occurrence in the brake system is more likely. An increase of disc thickness causes the elevation of the critical velocity value and reduces probability of TMI occurrence.
- In the analysed industrial brakes, it is more likely that the permissible value of stress is going to be locally exceeded than the permissible value of the axial distortion of the disc.

REFERENCES

1. Anderson A.E., Knapp R.A.: Hot spotting in automotive friction systems. Wear, 1990, 135, 319–337.
2. Kao T.K., Richmond J.W.: Brake disc hot spotting and thermal judder. Int. Journal of Vehicle Design, 2000, 23, 276–295.
3. Ścieszka S.F.: Fricion Brakes (in polish). WZP – ITeE, Radom 1998.
4. Barber J.R.: Elasticity, Kluwer Academic Publishers, Boston 1992.
5. Yi Y., Barber J.R., Zagrodzki P.: Eigenvalue solution of thermoelastic instability problems using Fourier reduction. Proc. Roy. Soc. A 456, 2000, 2799–2821.
6. Panier S., Dufrenoy P., Weichert D.: An experimental investigation of hot spots in railway disc brakes. Wear, 2004, 256, 764–773.
7. Ji-Hoon, Choi Lee: Finite element analysis of transient thermoelastic behaviours in disc brakes, Wear, 2004, 257, 47–58.
8. Yevtuschenko A.A., Grześ P.: The FEM – modeling of the frictional heating phenomenon in the pad/disc tribosystem (a review), Numerical Heat Transfer, Part A, vol. 58, No 3, 2010, 207–226.
9. Grześ P.: Finite element analysis of disc temperature during braking process, Acta Mechanica et Automatica, 2009, 4, 36–42.
10. Grześ P.: Finite element analysis of temperature distribution in axisymmetric model of disk brake, Acta Mechanica et Automatica, 2010, 4, 23–28.
11. Żołnierz M.: The effect of the winder disc brake's design feature on its thermoelastic instability. PhD thesis (in polish). Silesian University of Technology, Gliwice, 2006.
12. Ścieszka S.F., Żołnierz M.: The effect of the winder disc brake's design feature on its thermoelastic instability Part 1. Set-up for finite element modeling and numerical model verification, ZEM, 2007, 3, 111-124.

13. Ścieszka S.F., Żołnierz M.: The effect of the winder disc brake's design feature on its thermoelastic instability Part 2. Finite element simulation, ZEM, 2007, 4, 183–193.
14. Kowal L., Turewicz K., Kruczek T.: Temperature measurement in mine winder's disc brake, Maszyny Górnicze 2/2012, 3–12.
15. Grzegorzek W., Ścieszka S.F.: Prediction on friction characteristics of mine hoist disc brakes using artificial neural networks, Scientific Problems of Machines Operation and Maintenance, ZEM, 2011, 46, 27–42.
16. Zhen-cai Zhu, Yu-xing Peng, Zhi-yuan Guo-an Chen.: Three-dimension transient temperature field of brake shoe during hoist's emergency braking. Applied Thermal Engineering, 2009, 29, 932-937.
17. Farren S.W., Taylor G.I.: The heat developed during plastic extension of metals. Proceedings of the Royal Society, 1925, 107, 422.
18. Komanduri R., Hou Z.B.: Analysis of heat partition and temperature distribution in sliding systems, Wear, 251, 2001, 925–938.
19. Christie I., Griffiths D.F., Michell A.R., Zienkiewicz O.C.: Finite element methods for second order differential equations with significant first derivatives. International Journal for Numerical Methods in Engineering, 1976, 10, 1389–1396.
20. Yu C.C., Heinrich J.C.: Petrov – Galerkin methods for multidimensional time – dependent convective transport equation. International Journal for Numerical Methods in Engineering, 1987, 2201–2215.

Streszczenie

Artykuł przedstawia wyniki badań rozkładu temperatur na powierzchni tarczy hamulcowej w czasie hamowania awaryjnego maszyny z użyciem kamery termowizyjnej. Uzyskane wyniki umożliwiły weryfikację obliczeń numerycznych tego procesu hamowania. Przedstawiono także badania tribologiczne charakterystyki ciernej pary hamulcowej, czyli materiału okładziny hamulcowej i materiału tarczy hamulcowej. Badania tribologiczne wykonano na stanowisku spełniającym najważniejsze kryteria podobieństwa do hamulca tarczowego maszyny wyciągowej. Uzyskane wartości współczynników tarcia kinetycznego i statycznego były wykorzystane następnie w modelowaniu numerycznym termomechanicznej niestabilności analizowanego hamulca i wyznaczeniu krytycznej prędkości początkowej, powyżej której system staje się niestabilny. Obliczenia numeryczne obejmowały także wyznaczenie naprężeń termicznych w tarczy, deformacji osiowej tarczy oraz wpływu podziału tarczy na segmenty na naprężenia i jej deformacje osiowe.